2010 American Control Conference
Marriott Waterfront, Baltimore, MD, USA
June 30-July 02, 2010

Robust Adaptive Control of the Mold Level in the Continuous Casting Process Using Multiple Models

K. Jabri, E. Godoy, D. Dumur, A. Mouchette, and B. Bèle

Abstract—**In the continuous casting of steel, mold level control is fundamental for obtaining high productivity and high quality. Using conventional methods, it is difficult to achieve both stability and performance robustness because of different classes of disturbances and parameters uncertainties in the process. This paper presents a multi-model adaptive control architecture based on the so-called RMMAC methodology. With the help of precise definition of robust performance requirements, the number of models, estimators and controllers are merely derived. More importantly, the combination of robust non-adaptive mixed-μ synthesis and stochastic hypothesis testing concepts enables controller performances prediction as well as online monitoring process parameters which could be used by operators to take corrective actions. The generated signals are likewise useful for understanding the physical phenomena in the process.**

I. Introduction

TODAY, most of the 750 million tons of steel produced in the world every year have been solidified using the continuous casting process. Because of its higher productivity and lower costs, it has become a worldwide technology in the steel industry. Fig. 1 shows an example of the caster configuration. Referring to this figure, molten steel flows out of the ladle into the mold through a refractory called the tundish. The solidification begins in the mold and continues in the secondary cooling zone producing thereby a strand with a solid outer shell and a liquid core. This strand passes then through the withdrawal rolls and becomes fully solidified at the caster exit where it is cut into pieces of predetermined lengths, called the slabs.

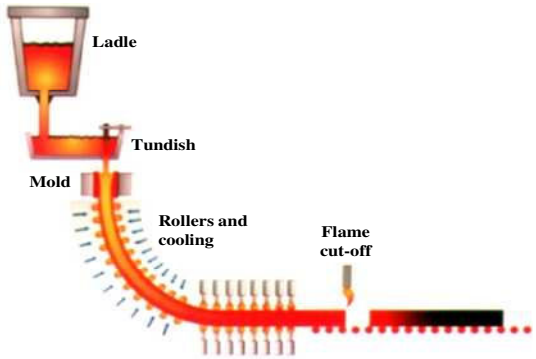

Fig. 1. Continuous casting machine side view

K. Jabri, A. Mouchette and B. Bèle are with the Measurement and Control Department of ArcelorMittal Global Research and Development, Maizières-Lès-Metz, France (e-mail: karim.jabri@asso-supelec.org).

E. Godoy, D. Dumur are with SUPELEC Systems Sciences (E3S) - Automatic Control Department, Gif-sur-Yvette, France (e-mail: {emmanuel.godoy, didier.dumur}@supelec.fr).

Several studies have revealed that the quality of the slabs is greatly affected by fluid flow phenomena in the mold region of the process. Since the level fluctuations over the meniscus surface are one of them, the flow into the mold is always controlled by means of a stopper rod or a sliding gate. Except the transients in the process such as ladle changes, the casting speed is usually kept constant. The objective of the control system is to maintain a stable level in the mold using local measurements corrupted by noise.

This control problem becomes much harder when the process characteristics change suddenly or when unpredicted disturbances take place during the casting operations. The main one considered here is the bulging caused by increasing pressure inside the strand which deforms the solidified shell profile. The outcome of this phenomenon is huge mold level fluctuations whose spectrum is between 0.03 and 0.1Hz but depends on the casting speed and the roll pitch. Other sinusoidal disturbances act on the mold such as the standing waves. Their frequencies which are correlated with the mold geometry, appear to be in the range of 0.65 - 0.85Hz.

Numerous non-adaptive control strategies have been proposed. Some of them have been implemented in a few plants. Representative references cited in the literature are [1]-[5]. In this paper, we shall adopt a different approach based on multi-model architecture. We use the Robust Multiple Model Adaptive Control (RMMAC) method published recently [7]. In such control problem, it is highly desirable that the controller remains stable and also meets the posed performance specifications whatever the parameters variations. Several identification trials point out indeed that the casting parameters change slowly in time. RMMAC gives a solution to this concern. It significantly improves the bulging rejection compared with the best non-adaptive controller designed using the mixed-μ synthesis.

The paper is structured as follows. The next section describes the plant model classically used for mold level controller design. Section 3 defines the performance requirements for robust disturbance rejection and analyses the potential benefits of using adaptive control. In section 4, we present first the RMMAC concepts. Then, we describe how we divided the initial parameter uncertainty into smaller parameter subsets and designed the local robust controller and the Kalman filter for each model. Finally, section 5 presents various simulations confirming thus the positive aspects of the RMMAC method.

II. MOLD LEVEL DYNAMICS

The plant model is a single input single output system as depicted in Fig. 2. The control input P^* is the stopper position setpoint delivered by the main controller. An inner loop modeled here by a first order function with the time constant τ_a, controls the stopper position P which determines the flow into the mold Q_{in}. The flow out of the mold Q_{out} is imposed by the casting speed and the mold section S. The level N is then calculated from the integration of the difference between Q_{in} and Q_{out} divided by the mold section. The key parameters of the plant model are the stopper gain G_n and the nozzle delay τ_n because their values are not known precisely and may vary with the caster configuration.

Therefore, the process transfer function is given by the following equation where s is the Laplace variable:

$$H = \frac{N}{P^*} = \frac{G_n e^{-\tau_n s}}{Ss(1+\tau_a s)} = H_0 e^{-\tau_n s} \tag{1}$$

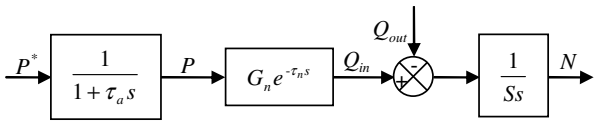

Fig. 2. Plant model

The time delay effect may be approximated by a first order Pade function leading to the following state-space formalism:

$$\begin{cases} \dot{x} = Ax + Bu \\ y = N = Cx + v_n \end{cases} \tag{2}$$

with:

$$\begin{cases} x^T = (N \quad P \quad q_p) \\ u^T = (Q_{out} \quad P^*) \\ q_p = G_n P(t-\tau_n) + G_n P(t) \end{cases} \tag{3}$$

$$A = \begin{pmatrix} 0 & -G_n/S & 1/S \\ 0 & -1/\tau_a & 0 \\ 0 & 4G_n/\tau_n & -2/\tau_n \end{pmatrix},\ B = \begin{pmatrix} -1/S & 0 \\ 0 & 1/\tau_a \\ 0 & 0 \end{pmatrix},\ C^T = \begin{pmatrix} 1 \\ 0 \\ 0 \end{pmatrix}$$

v_n is an additive white sensor noise whose intensity is defined as:

$$\mathrm{E}(v_n(t)v_n(t-\tau)) = V\delta(\tau)$$

In this work, this plant model is discretized at $T_s = 0.01\mathrm{s}$. The following parameters are fixed and known:

$$S = 0.3648\,\mathrm{m}^2,\ G_n = 1\mathrm{l/s/mm},\ V = 10^{-2}\,\mathrm{mm}^2 \tag{4}$$

For the unknown parameters τ_n and τ_a, only the ranges can be identified:

$$\begin{cases} \tau_n \in [0.1 \quad 2]\mathrm{s} \\ \tau_a \in [0.001 \quad 0.1]\mathrm{s} \end{cases} \tag{5}$$

III. PERFORMANCE SPECIFICATION AND ANALYSIS

This section analyses the control loop performances. This step is vital since it provides the designer with the information to decide whether to implement an adaptive control architecture [8].

A. GNARC design

From now on, we focus our attention to the problem of bulging rejection. As explained in the introduction, the bulging disturbance has a frequency band between 0.03 and 0.1Hz. The bulging effect on the level may be quantified using the average magnitude of the transfer function between the flow out the mold Q_{out} and the level N (TF_{bulge}) over the bulging frequency range. From a performance point of view, this average magnitude should be as small as possible. It is determined via mixed-μ synthesis [9] (known also as DG-K algorithm) leading to the best 'Global Non-adaptive Robust Compensator' GNARC. The mixed-μ synthesis theory is too abundant for a review in the framework of this paper. Further developments can be found in [10] and [11]. Since the plant model uncertainties are real, it is recommended to use the mixed-μ synthesis rather than the complex-μ synthesis (known also as D-K algorithm) which deals only with the complex uncertainties and may provide a conservative controller in our case. GNARC takes into account all the parameters uncertainties (τ_n and τ_a), the frequency weight which shapes the bulging rejection and the sensor noise. To compute GNARC, the basic idea is to find an initial weighting function so that the mixed-μ synthesis generates a controller with an upper bound $\mu(\omega)$ such as:

$$\mu(\omega) < 1 \quad \forall\omega \tag{6}$$

Therefore, the control loop is guaranteed stable for all the parameters uncertainties. At the same time, the posed performance requirements are met. GNARC is then determined by maximizing the performance parameter until the μ upper bound is just below the unity:

$$0 < 1 - \mu(\omega) < 10^{-2} \quad \forall\omega \tag{7}$$

GNARC is thereby the best possible robust performance we can expect in the absence of adaptation.

To carry out the mixed-μ synthesis, two weighting functions have been introduced:

Bulging rejection weight: $W_b = \dfrac{10.4 \cdot (s+0.314)(s+3.14)}{(s+0.0209)(s+314)}$

Measurement noise weight: $W_n = 0.01$

W_b is thus chosen to quantify the potential performance benefit over the bulging frequency band. Fig. 3 depicts the required diagram for the mixed-μ synthesis. The generalized plant includes the nominal plant dynamics and the frequency weights. The block Δ incorporates the normalized real parameters uncertainties. K is the stabilizing controller which guarantees the posed performance specifications for the entire unknown parameters intervals.

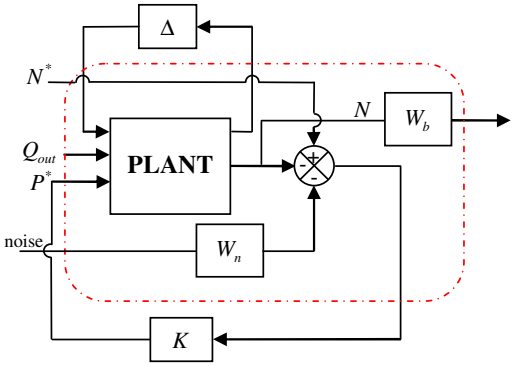

Fig. 3. Control scheme for μ design

The disturbance rejection criterion, used here to evaluate the quality of bulging rejection, is defined as follows:

$$Perf_{dB} = \frac{\left(\max_{\omega\in[0.03\ 0.1\text{Hz}]} \left|TF_{bulge}(j\omega)\right| + \min_{\omega\in[0.03\ 0.1\text{Hz}]} \left|TF_{bulge}(j\omega)\right| \right)}{2} \quad (8)$$

This gain is minimized (so that the bulging rejection performance is maximized) until the μ upper bound is equal to 0.993 (which is the best possible value we can obtain in our application). The largest performance was determined to be:

$$GNARC = 13.5\text{dB} \quad (9)$$

Results are illustrated in Fig. 4.

B. FNARC design

Prior to making any decision on using adaptive control, one needs to compute the other performance bound called the 'Fixed Non-Adaptive Robust Compensator' FNARC [7]. It is calculated assuming that the unknown parameter, here the delay τ_n, takes a known value of the range uncertainty. Using the same scheme as for GNARC design (Fig. 3), we define first a grid for the delay $\tau_n(i)$. For each fixed value $\tau_n(i)$, we minimize the performance parameter (8) until the inequality (7) is satisfied in order to determine the best robust controller.

In summary, the FNARC is the best possible performance that we may expect if the unknown parameter is identified exactly. Results are shown in Fig. 4 for comparison purposes.

C. Performances analysis

Following the procedures described previously, the performance bounds as functions of the delay τ_n are plotted in Fig. 4.

Clearly, if we know the delay exactly, we can improve significantly the bulging rejection performance from 13.5dB to a range between -1.55 and 12.1dB. This agrees with the engineering intuition.

Furthermore, the performance seems to be higher if the delay is near its lower bound 0.1s. The benefit of using adaptive control is obvious in this region. However, it decreases in the other side of the delay interval where the best expected performance is 12.1dB which is closer to the GNARC value (13.5dB).

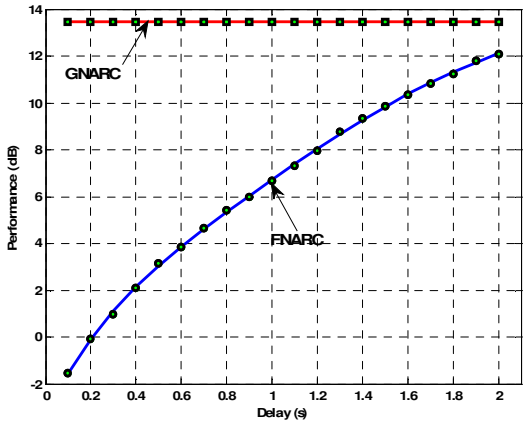

Fig. 4. Best GNARC and FNARC performance in dB for delay uncertainty

In order to agree with the notations already introduced in [7], the performance parameter is formulated as follows:

$$A_p = \frac{1}{10^{Perf_{dB}/20}} \quad (10)$$

Based on this definition, A_p should be as large as possible for superior bulging rejection. GNARC provides thereby the performance lower bound while the FNARC provides its upper bound (Fig. 5). This figure shows that the performance may be improved about $1.2/0.21 = 5.7$ times by using adaptive control for lower values of the delay.

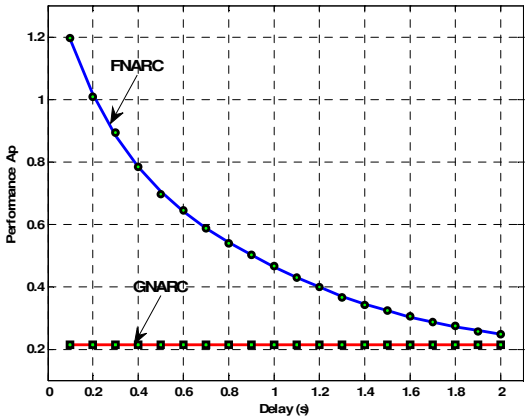

Fig. 5. Best GNARC and FNARC performance for delay uncertainty

To summarize the underlying results, the analysis above reveals that there is a meaningful benefit in using adaptive control, in particular the multiple model architecture. In the sequel, the RMMAC method is investigated and implemented. It is noteworthy to mention that the GNARC and FNARC curves are to be used as the performance comparison basis as well as a useful tool to obtain the RMMAC models which cover the whole initial uncertainty set.

IV. RMMAC METHODOLOGY

The previous section indicates that our case study will benefit from adaptive control strategy. By decreasing the delay uncertainty interval, it is indeed possible to improve the bulging rejection. There are several approaches for adaptive control. The vast majority of them deal with the case of constant uncertain real parameters. In the case of mold level control, the delay is uncertain and may vary depending on caster configuration. Such control problem has been addressed in [12] which developed a robust adaptive control method so-called Robust Multiple Model Adaptive Control (RMMAC). In this section, we evaluate the bulging rejection performance of the RMMAC architecture compared to the best non-adaptive controller designed using the mixed-μ synthesis (GNARC).

A. *RMMAC architecture*

The RMMAC architecture is shown in Fig. 6 where the PLANT block is the transfer between the stopper position setpoint and the level (Fig. 2). This architecture uses a set of controllers and Kalman filters. Each local controller generates a local control input $u_j(t)$. Kalman filters are only used to generate residuals $r_j(t)$ (in the Kalman filter theory, the residual or the innovation is the discrepancy between the actual and the predicted values of the measurement) contrary to other multiple model structures where the Kalman filters state estimates are used to generate the control signals. These residuals are then utilized by the Posterior Probability Evaluator block (PPE) which calculates online the posterior conditional probability $P_j(t)$ that each model generates the plant output. The global control input $u(t)$ is finally computed by weighting each local control signal with its associated posterior probability, as follows:

$$u(t) = \sum_{j=1}^{n} P_j(t) u_j(t) \qquad (11)$$

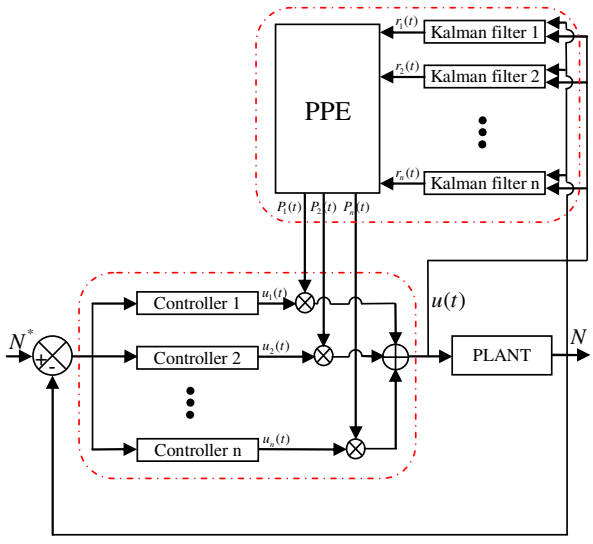

Fig. 6. RMMAC architecture

There are two key elements of RMMAC:

i. The choice of the number of models m. It is determined using the GNARC and FNARC designs and the mixed-μ synthesis. The associated software generates the set of 'Local Non-Adaptive Robust Compensators' LNARCs as well (IV.B).

ii. The design of Kalman filters. A nominal value of the delay should be determined for each model to construct the associated Kalman filter. It is computed using the Baram Proximity Measure (BPM) to ensure the convergence of the posterior probabilities (IV.C).

B. *Designing multiple models and local controllers*

Like any adaptive multiple model architecture, the number of models required by RMMAC depends on performance specifications. It is derived by decreasing only the delay uncertainty set. As explained in [12], this number is obtained so that the achieved performance should be equal or exceed an imposed limit. Since the FNARC represents the performance upper bound, we may specify this limit to be X% of FNARC. In this work, we used the value X=60 (Fig. 7). Following the algorithm described in [12], we start at the lower bound of the delay 0.1s where the FNARC is maximum. We increase then the uncertainty set and we calculate the associated maximum performance parameter A_p using the mixed-μ synthesis. This leads to the dashed curve. We iterate this calculation as long as the performance parameter is greater than the maximum of 60% FNARC. As a result, the upper bound of the first subset lies at the intersection of the dashed curve and the maximum of the 60% FNARC curve. This algorithm yields both first subset and first controller (LNARC1). The results are summarized in TABLE I.

This process is then repeated starting from the upper bound of the first subset until the delay upper bound is reached. At the end of this process, five subsets have been identified in order to achieve a performance greater than 60% FNARC over the whole initial uncertainty set (Fig. 7). Higher performance requires naturally more models.

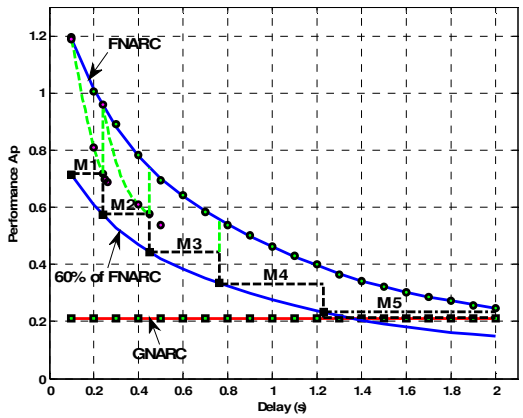

Fig. 7. Definition of models bounds and LNARCs

TABLE I
COMPARISON BETWEEN LNARC AND GNARC PERFORMANCES

Controller	A_p	μ_{ub}	Subset
1	0.718	0.994	[0.1, 0.24]
2	0.577	0.995	[0.24, 0.45]
3	0.444	0.991	[0.45, 0.76]
4	0.333	0.988	[0.76, 1.23]
5	0.215	0.988	[1.23, 2]
GNARC	0.212	0.993	[0.1, 2]

TABLE I compares the expected performance in each subset with the GNARC one. Clearly, one should expect better bulging rejection especially for lower values of the delay.

C. Designing the set of Kalman filters

Now that the number of models and the associated controllers have been derived, we turn our attention to the identification part of the RMMAC architecture which requires the design of m Kalman filters ($m = 5$ in our case) and the Posterior Probability Evaluator (PPE). The uncertainties of the actuator time constant τ_a are ignored in the Kalman filters design. Therefore, the only remaining parameter required to design a Kalman filter is the delay. A numerical value should be identified in each subset using the Baram Proximity Measure [13] or the Kullback information metric [14]. This process determines thereby m values leading to the following m discrete time state-space dynamics:

$$\begin{cases} x_k(n+1) = A_k x_k(n) + B_k u(n) + L_k w(n) \\ y_k(n) = C_k x_k(n) + v(n) \end{cases} \tag{12}$$

where $k = 1,\ldots,m$ and $n = 0,1,\ldots$ refer to the model and the time index respectively. $\{w(n)\}$ and $\{v(n)\}$ represent the process and the measurement noise respectively. They are assumed to be white gaussian sequences, uncorrelated with $x_k(0)$ and independent of each other with:

$$\begin{cases} \mathrm{E}(w(n)w(n)^T) = Q_k \\ \mathrm{E}(v(n)v(n)^T) = R_k \end{cases} \tag{13}$$

The notation used in the sequel is fairly standard:

$$\hat{x}_k(n/n) = \mathrm{E}(x_k(n)/u(0)\cdots u(n-1), y(1)\cdots y(n)) \tag{14}$$

$$\Phi_k(n/n) = \mathrm{E}((x_k(n) - \hat{x}_k(n/n))(x_k(n) - \hat{x}_k(n/n))^T / u(0)\cdots u(n-1), y(1)\cdots y(n)) \tag{15}$$

As it is frequently the case, the steady state Kalman filter is computed using the two following cycles:

Predict cycle:

$$\begin{cases} \hat{x}_k(n+1/n) = A_k \hat{x}_k(n) + B_k u(n) \\ \hat{y}_k(n+1/n) = C_k \hat{x}_k(n+1/n) \\ r_k(n+1) = y(n+1) - \hat{y}_k(n+1/n) \end{cases} \tag{16}$$

$$\begin{cases} \Phi_k^p = A_k \Phi_k A_k^T + L_k Q_k L_k^T \\ S_k = \mathrm{cov}(r_k(n+1), r_k(n+1)) = C_k \Phi_k^p C_k^T + R_k \end{cases} \tag{17}$$

Update cycle:

$$\begin{cases} K_k = \Phi_k^p C_k^T S_k^{-1} \\ \Phi_k = \Phi_k^p - \Phi_k^p C_k^T S_k^{-1} C_k \Phi_k^p \end{cases} \tag{18}$$

$$\hat{x}_k(n+1/n+1) = \hat{x}_k(n+1/n) + K_k r_k(n+1) \tag{19}$$

The fact that one of the m models is the true one, i.e. the one which is generating the plant output, is modeled by a hypothesis random variable H_k. At initial time, the hypothesis H_k are assumed equiprobable, i.e.:

$$P_k(0) = \mathrm{Prob}(H = H_k) = \frac{1}{m} \tag{20}$$

The posterior probabilities $P_k(n)$ are defined as follows:

$$P_k(n) = \mathrm{Prob}(H = H_k / u(0)\cdots u(n-1), y(1)\cdots y(n)) \tag{21}$$

They must satisfy: $P_k(n) \geq 0, \sum_{k=1}^{m} P_k(n) = 1$ (22)

Using Bayes rule and assuming that the model set includes the true plant, we obtain [15]:

$$P_k(n+1) = \frac{p(y(n+1)/u(n), H_k, Y(n))}{p(y(n+1)/u(n), Y(n))} P_k(n) \tag{23}$$

with: $Y(n) = (u(0)\cdots u(n-1), y(1)\cdots y(n))$

Furthermore, $p(y(n+1)/u(t), H_k, Y(n))$ is gaussian whose mean is:

$$\mathrm{E}(y(n+1)/u(n), H_k, Y(n)) = C_k \hat{x}_k(n+1/n) \tag{24}$$

and steady state covariance is:

$$\mathrm{cov}(y(n+1), y(n+1)/u(n), H_k, Y(n)) = C_k \Phi_k^p C_k^T + R_k = S_k \tag{25}$$

We deduce that:

$$p(y(n+1)/u(n), H_k, Y(n)) = \frac{1}{\sqrt{2\pi \det(S_k)}} e^{-\frac{1}{2} r_k(n+1) S_k^{-1} r_k(n+1)} \tag{26}$$

Moreover, using the marginal density and the Bayes rule once more, we obtain:

$$p(y(n+1)/u(n), Y(n)) = \sum_{i=1}^{m} P_i(n) p(y(n+1)/u(n), H_i, Y(n)) \tag{27}$$

In closing, we deduce from equations (23), (26) and (27) the general recursive formula of the posterior probabilities, which is computed on line by the Posterior Probability Evaluator (PPE) (Fig. 6):

$$\begin{cases} P_k(n+1) = \\ \dfrac{\dfrac{1}{\sqrt{2\pi\det(S_k)}} e^{-\frac{1}{2} r_k(n+1) S_k^{-1} r_k(n+1)}}{\sum_{i=1}^{m} P_i(n) \dfrac{1}{\sqrt{2\pi\det(S_i)}} e^{-\frac{1}{2} r_i(n+1) S_i^{-1} r_i(n+1)}} P_k(n) \\ P_k(0) = \dfrac{1}{m} \end{cases} \quad (28)$$

We stress that the above results are valid only if the true plant is assumed to belong to the model set. If it is not the case, the identification subsystem of the RMMAC architecture should converge to the closest model of the set in an information metric sense. The proper way of determining the nominal values of the delay τ_n^k in each subset is based on a probabilistic distance between different stochastic systems. It is noteworthy to mention that the strategy consisting to choose τ_n^k at the centers of subsets leads to unpredictable behaviors of the posterior probabilities. In this work, τ_n^k are selected using the Baram Proximity Measure (BPM) denoted by $L(\tau_n, \tau_n^k)$ which measures the stochastic distance between the residuals $r(n)$ and $r_k(n)$. Convergence of posterior probabilities is guaranteed by the following theorem [13].

Let M^* denotes the whole model set which includes the nominal values τ_n^k and the true plant, denoted by $*$.

Theorem [13]**:** Under the following assumptions:

i. $[x(n)]$ is stationary i.e., for every F belonging to the σ - algebra of Borel sets of $R^3 \times R^3 \times \cdots$, we have:

$$P[x(1), x(2), \ldots, x(n) \in F] = P[x(l+1), x(l+2), \ldots, x(l+n) \in F] \quad (29)$$

ii. $[x(n)]$ is ergodic, i.e.

$$\lim_{n\to\infty} \frac{1}{n+1} \sum_{l=0}^{n} \left| \mathrm{E}(x(n) x^T(n+l)) \right|^2 = 0 \quad (30)$$

iii. For each $i \in M^*$, the residual covariance S_i exists and has a finite positive definite value.

iv. For each $i \in M^*$, the residual sequence $[y(n) - \hat{y}_i(n)]$ is ergodic.

If the BPMs satisfy the inequality

$$L(\tau_n, \tau_n^i) \prec L(\tau_n, \tau_n^k) \quad \forall k \neq i \quad (31)$$

Then, the posterior probabilities converge almost surely to the correct model, i.e. $\lim_{n\to\infty} P_i(n) \to 1$ (32)

Therefore, τ_n^k should be obtained so that the BPMs agree at the boundary of adjacent models. In this manner, the posterior probability of the closest model to the true plant (the one with the smallest BPM) will converge almost surely to unity.

All the stationarity and ergodicity conditions are important and must be satisfied [16], [17]. If it is not the case, one might use a fake white noise to robustify the Kalman filters [18], [19].

We now focus on the BPM. In the sequel of this section, we shall briefly present all needed equations to compute this distance.

Let us first establish some notation. For $i, j \in M^*$, define:

$$\Gamma_j^i = E\left\{ \left[y(n) - \hat{y}_j(n) \right] \left[y(n) - \hat{y}_j(n) \right]^T / H_i \neq H_j \right\}$$

$$A_j^i = \begin{pmatrix} A_i & 0 \\ A_j K_j C_i & A_j (I - K_j C_j) \end{pmatrix}$$

$$L_j^i = \begin{pmatrix} L_i & 0 \\ 0 & A_j K_j \end{pmatrix}, \; Q^i = \begin{pmatrix} Q_i & 0 \\ 0 & R_i \end{pmatrix}, \; C_j^i = \begin{pmatrix} H_i & -H_j \end{pmatrix}$$

$$\Psi_j^i(n) = E\left\{ \begin{bmatrix} x_i(n) \\ \hat{x}_j(n) \end{bmatrix} \begin{bmatrix} x_i(n) \\ \hat{x}_j(n) \end{bmatrix}^T \right\}$$

It can be shown that $\Psi_j^i(n)$ is generated by:

$$\Psi_j^i(n+1) = A_j^i \Psi_j^i(n) A_j^{i\,T} + L_j^i Q^i L_j^{i\,T} \quad (33)$$

Its steady state Ψ_j^i is finite if A_j^i has all its eigenvalues inside the unit cycle. It may be determined by solving the Lyapunov equation:

$$\Psi_j^i = A_j^i \Psi_j^i A_j^{i\,T} + L_j^i Q^i L_j^{i\,T} \quad (34)$$

Ψ_j^i is useful to calculate Γ_j^i. It can be proven indeed that:

$$\Gamma_j^i = C_j^i \Psi_j^i C_j^{i\,T} + R_i \quad (35)$$

For $k, j \in M^*$, let $I_n(k, j)$ denotes the mean information in $y(n)$ favoring model k against model j. It is defined by:

$$I_n(k, j) = \mathrm{E}\left\{ \log \frac{p(y(n)/H_k, Y(n-1))}{p(y(n)/H_j, Y(n-1))} \right\} \quad (36)$$

where $\mathrm{E}\{\}$ is the mean function.

From (26), we have:

$$\mathrm{E}\{\log p(y(n)/H_k, Y(n-1))\} = \frac{-1}{2} \log 2\pi - \frac{1}{2} \log|S_k| - \frac{1}{2} \mathrm{trace}(S_k^{-1} \Gamma_k^*) \quad (37)$$

For every $i \in M^*$, the Baram Proximity Measure of the jth subset is defined by:

$$L_j^i = \log|S_j| + \mathrm{trace}(S_j^{-1} \Gamma_j^i) \quad (38)$$

Therefore,

$$I_n(k, j) = \frac{1}{2} \log|S_j| + \frac{1}{2} \mathrm{trace}(S_j^{-1} \Gamma_j^*) - \frac{1}{2} \log|S_k| - \frac{1}{2} \mathrm{trace}(S_k^{-1} \Gamma_k^*) \quad (39)$$

and $I_n(k,j)=\frac{1}{2}(L_j^*-L_k^*)$ (40)

Also, $I_n(k,j)\geq 0$ if and only if $L_j^*\geq L_k^*$ (41)

If such parameter k exists, this means that the true plant is closer to the k[th] model ($I_n(k,j)\geq 0$). Hence, the corresponding posterior probability will converge to 1, since (31) holds.

V. SIMULATION RESULTS AND PERFORMANCE EVALUATION

In this section, we present some representative simulation results which evaluate the benefits of using RMMAC when the delay is uncertain. Because of its advanced structure, many aspects should be investigated. Hence, several significant scenarios have been tested. They are not all explicitly shown in this paper due to space limitations.

In the mold level control simulator developed with parameters issued from a real plant, the bulging is modeled by a sine wave whose frequency is 0.03Hz or 0.05Hz. Following the procedure described in the previous section, the numerical values of the delay are determined so that the BPMs agree at the boundary of adjacent models. They are:

$$\tau_n \in \{0.15, 0.3, 0.65, 1, 1.5\} \quad (42)$$

Among the numerous simulations done, three cases have been considered (TABLE II). In each case, the dynamic behaviors of the five posterior probabilities are plotted as well as the level when the bulging occurs. Fig. 9, 11 and 13 compare the performance of the non-adaptive controller (GNARC) to that of the RMMAC. The other controllers currently used in plants are not stable over the whole delay uncertainty and cannot thereby be compared to RMMAC.

TABLE II
DELAY VALUES OF THE TRUE PLANT

Case	τ_n	Comment
1	0.15	Constant value among the nominal values
2	0.8	Random constant value
3	{0.6, 1.5, 1, 0.2}	Random sequence stair

Obviously, the adequate model is identified in a few seconds and the improvement in bulging rejection by the RMMAC is clear. In case 2, we have convergence to model 4 even though the euclidean distances indicate the opposite ($|\tau_n^*-\tau_n^3|<|\tau_n^*-\tau_n^4|$). This is because calculations show that $L(\tau_n^*,\tau_n^4)<L(\tau_n^*,\tau_n^3)$ ($\tau_n^*=0.8$ belongs to subset 4).

On the other hand, the performances improvement is much better for lower values of the delay as expected (TABLE I).

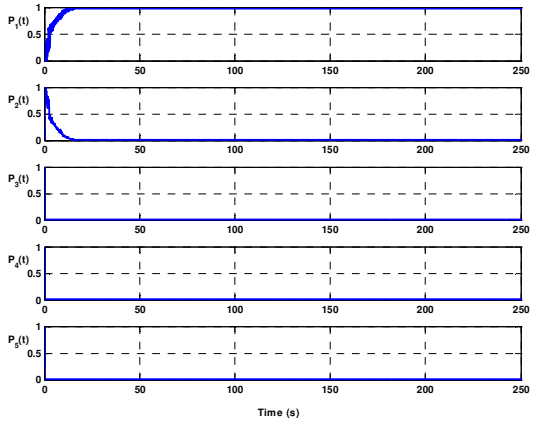

Fig. 8. Posterior probabilities (case 1)

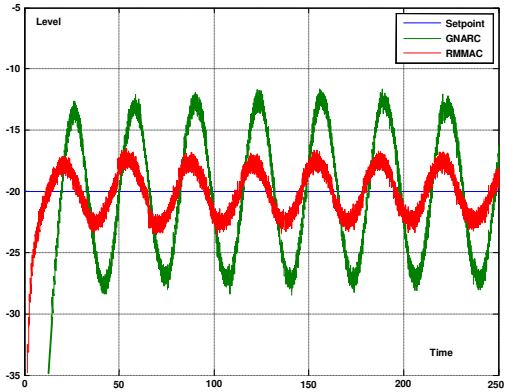

Fig. 9. Performance comparison between RMMAC and GNARC (case 1)

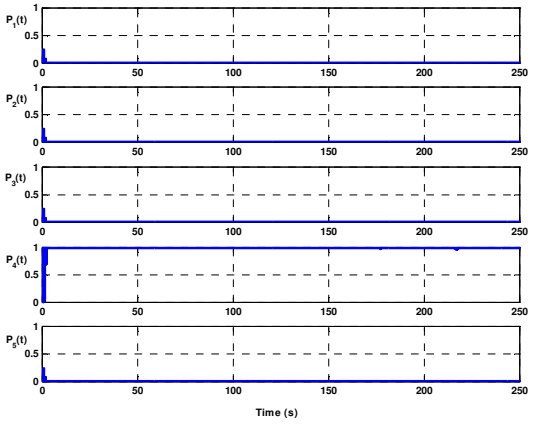

Fig. 10. Posterior probabilities (case 2)

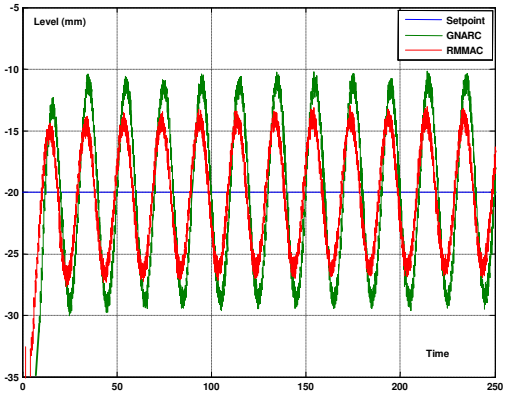

Fig. 11. Performance comparison between RMMAC and GNARC (case 2)

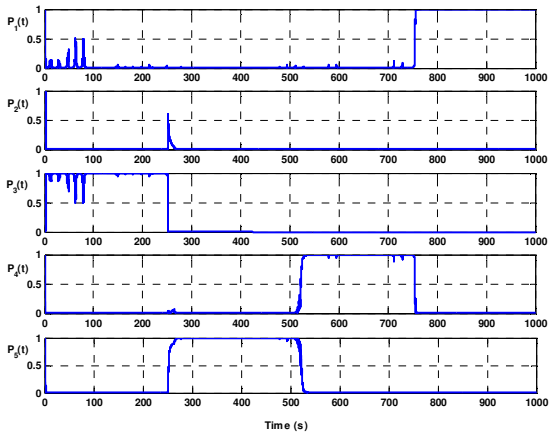

Fig. 12. Posterior probabilities (case 3)

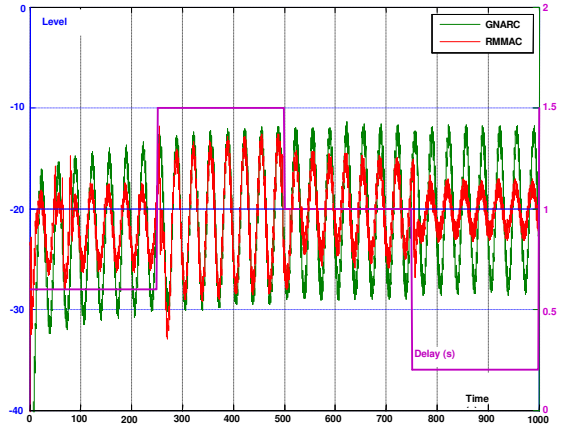

Fig. 13. Performance comparison between RMMAC and GNARC (case 3)

In real plant, delay changes slowly in time. The case 3 evaluates the RMMAC performance when the delay is assumed to vary according to a sequence stair chosen arbitrary in the whole uncertainty set. Once more, RMMAC yields superior bulging rejection.

VI. Conclusion

This paper presented a robust solution to the mold level control problem, which hinges upon the most recent progress on adaptive control. Contrary to other multiple models strategies, this methodology so-called RMMAC takes advantage of the mixed-μ synthesis to design multiple controllers for smaller parameter uncertainties so that an imposed performance is achieved. Furthermore, it enables the prediction of the expected performance benefit in the specified frequency region by using RMMAC instead of a robust controller. To get better performance, more models are undoubtedly required.

Since the RMMAC architecture is well documented only for a single scalar parameter, we have considered a unique uncertain real parameter which is the delay in the plant state-space description. The integration of the gain uncertainties in the RMMAC design is currently our topic of research. In such multiple uncertain parameter cases, the GNARC, FNARC and BPM become surfaces. Although the calculations are somewhat burdensome, the same philosophy still applies to determine the minimum number of models as well as in the definition of the nominal values for designing the Kalman filters.

Finally, from an operating point of view, this structure may provide valuable insights about the flow phenomena in the mold region by means of posterior probabilities which pinpoint the locations of process parameters.

Acknowledgment

Karim Jabri hereby expresses his deep gratitude to Prof. Gary Balas, the Aerospace Engineering and Mechanics Head Department of University of Minnesota, who provided him with the latest version of the mixed-μ software [9] which is at the heart of RMMAC design.

References

[1] Y. Matoba, T. Yamamoto, M. Tozuda, T. Watanabe, H. Tomono, "Instrumentation and control technology for supporting high-speed casting", 9th Process Technol. Conf. Proc., pp. 101-109, 1990.

[2] H. Kitada, O. Kondo, H. Kusachi, K. Sasame, "H_∞ control of molten steel level in continuous caster", IEEE Trans. on Control Systems Technology, 6(2), pp. 200-207, 1998.

[3] K. Jabri, A. Mouchette, B. Bèle, D. Dumur, E. Godoy, "Suppression of periodic disturbances in the continuous casting process", in *Proc. of Multi-conference on Systems and Control MSC-CCA*, San Antonio, 2008.

[4] K. Jabri, D. Dumur, E. Godoy, A. Mouchette, B. Bèle, "Modified Smith predictor scheme for periodic disturbances reduction in the continuous casting process", in *Proc. of Asian Control Conference ASCC*, Hong Kong, 2009.

[5] C. Furtmueller, E. Gruenbacher, "Suppression of periodic disturbances in continuous casting using an internal model predictor", in *Proc. of International Conference on Control Applications*, Munich, Germany, 2006.

[6] D. Suzuki, "Formulation of mold level control model by molten steel flow analysis method", Nippon steel technical report n° 89, 2004.

[7] M. Athans, S. Fekri, A. Pascoal, "Issues on robust adaptive feedback control", *Invited plenary paper, in Preprints 16th IFAC World Congress*, pp. 9-39, July 2005.

[8] S. Fekri, M. Athans, A. Pascoal, "RMMAC: a novel robust adaptive control scheme – Part 1: Architecture", in *Proc. of the IEEE Conf. on Decision and Control*, pp. 1134-1139, Bahamas, 2004.

[9] G.J. Balas, Private communication re mixed-μ software, 2009.

[10] P.M. Young, "Controller design with mixed uncertainties", in *Proc. of the American Control Conf.*, pp. 2333-2337, Baltimore, June 1994.

[11] P.M. Young, M.P. Newlin, J.C. Doyle, "μ analysis with real parametric uncertainty", in *Proc. of the IEEE Conf. on Decision and Control*, pp. 1251-1256, 1991.

[12] S. Fekri, "Robust adaptive MIMO control using multiple-model hypothesis testing and mixed-μ synthesis", Ph.D. thesis, Instituto Superior Técnico, Lisbon, Portugal, 2005.

[13] Y. Baram, "Information, consistent estimation and dynamic system identification", Ph.D. dissertation, MIT, Cambridge, MA, USA, 1976.

[14] B. Anderson and J. Moore, *Optimal filtering*. NJ, USA: Englewood Cliffs, Prentice-Hall, 1979.

[15] M. Athans and C. Chang, "Adaptive estimation and parameter identification using multiple model estimation algorithms", MIT Lincoln Lab., Lexington, MA, USA, 1976.

[16] J. Doob, *Stochastic Processes*. John Wiley & Sons, Inc., 1953.

[17] P. Halmos, *Lectures on Ergodic Theory*. Chelsea Publ. Co., 1956.

[18] M. Grewal and A. Andrews, *Kalman filtering*. Prentice-Hall, 1993.

[19] M. Grewal *et al.*, *Global Positioning Systems, Inertial Navigation, and Integration*. John Wiley & Sons, Inc., 2001.